

文章编号: 1674-8085 (2023) 02-0030-08

# A SUPRAMOLECULAR COMPLEX OF 5-NITRO-ISOPHTHALIC ACID AND PHEN MIXED LIGANDS: CHARACTERIZATION, PHOTOLUMINESCENT AND ELECTROCHEMICAL PROPERTIES

HUANG Jing-Ping<sup>1,2,\*</sup>, GUO Jin<sup>1</sup>, LIU Ruo-Lan<sup>1</sup>, CHEN Fei<sup>1</sup>, WU Wen-Chi<sup>1</sup>, WANG Zi-Yang<sup>1</sup>, HU Yu-Tao<sup>1</sup>, SUN Wu-Ni-Er<sup>1</sup>

(1. School of Chemistry and Chemical Engineering, Jinggangshan University, Ji'an, Jiangxi 343009, China;

2. Jiangxi Ganfeng Li Energy Technology Co., Ltd., Xinyu, Jiangxi 338000, China)

**Abstract:** A copper supramolecular complex with mixed ligands,  $[\text{CuClPhen}]^+ \cdot [\text{HL}]^- \cdot 2\text{H}_2\text{O}$  ( $\text{H}_2\text{L}$  = 5-Nitro-isophthalic acid, Phen = 1,10-phenanthroline) has been synthesized by a hydrothermal approach and its structure was determined by single-crystal X-ray crystallography. The title copper complex crystallizes in triclinic space group  $P-1$ . Crystal data for the title complex:  $\text{C}_{32}\text{H}_{24}\text{ClN}_5\text{CuO}_8$ ,  $M_r = 704.54$ ,  $a = 10.4044(5)$ ,  $b = 12.3912(9)$ ,  $c = 12.4632(9)$  Å,  $\alpha = 73.859(6)$ ,  $\beta = 85.036(5)$ ,  $\gamma = 78.202(5)^\circ$ ,  $V = 1510.09(17)$  Å<sup>3</sup>,  $Z = 2$ ,  $T = 293(2)$  K,  $D_c = 1.549$  g/cm<sup>3</sup>,  $\mu(\text{MoK}\alpha) = 0.874$  mm<sup>-1</sup>,  $F(000) = 720.0$ ,  $R = 0.0554$ ,  $wR = 0.1434$ , and  $GOF = 1.098$ . When used as the electrode material of the super-capacitors, the as-prepared complex showed high specific capacitance, good cycle stability and excellent rate performance. Specifically, the maximum specific capacitance can achieve 69 F/g in 1 mol/L KOH solution. At the current density of 2 A/g, the retention of specific capacitance was 72% after 10000 cycles. The title complex is a potential red photoluminescent material.

**Key words:** preparation; characterization; photoluminescence; electrochemical properties; copper complex

CLC number: O641

Document Code: A

DOI: 10.3969/j.issn.1674-8085.2023.02.005

## 一种含 5-硝基间苯二甲酸和菲咯啉配体的超分子化合物: 结构表征, 光致发光和电化学性能

黄敬平<sup>1,2,\*</sup>, 郭瑾<sup>1</sup>, 刘若兰<sup>1</sup>, 陈斐<sup>1</sup>, 吴文弛<sup>1</sup>, 王子扬<sup>1</sup>, 胡于涛<sup>1</sup>, 孙乌尼尔<sup>1</sup>

(1. 井冈山大学化学化工学院, 江西, 吉安 343009; 2. 江西赣锋锂电科技股份有限公司, 江西, 新余 338000)

**摘要:** 采用水热法合成了含混合配体的铜配合物  $[\text{CuClPhen}]^+ \cdot [\text{HL}]^- \cdot 2\text{H}_2\text{O}$  ( $\text{HL}$  = 5-硝基间苯二甲酸, Phen = 1,10-菲咯啉), 其结构由单晶 X 射线晶体学确定。标题化合物在三斜空间群  $P-1$  的晶体化合物。标题化合物的晶体数据:  $\text{C}_{32}\text{H}_{24}\text{ClN}_5\text{CuO}_8$ ,  $M_r = 704.54$ ,  $a = 10.4044(5)$ ,  $b = 12.3912(9)$ ,  $c = 12.4632(9)$  Å,  $\alpha = 73.859(6)$ ,  $\beta = 85.036(5)$ ,  $\gamma = 78.202(5)^\circ$ ,  $V = 1510.09(17)$  Å<sup>3</sup>,  $Z = 2$ ,  $T = 293(2)$  K,  $D_c = 1.549$  g/cm<sup>3</sup>,  $\mu(\text{MoK}\alpha) = 0.874$  mm<sup>-1</sup>,  $F(000) = 720.0$ ,  $R = 0.0554$ ,  $wR = 0.1434$ ,  $GOF = 1.098$ 。当用作超级电容器电极材料时, 所制备的配合物具有高比电容、良好的循环稳定性和优良的倍率性能。在 1 mol/L KOH 溶液中, 最大比电容可达到 69 F/g。在 2 A/g 电流密度下, 10000 次循环后比电容保持率为 72%。标题化合物是一种潜在的红色光致发光材料。

**关键词:** 超分子化合物; 晶体结构; 电化学性能

中图分类号: O641

文献标识码: A

DOI: 10.3969/j.issn.1674-8085.2023.02.005

Received date: 2022-04-06; Modified date: 2022-08-12

Foundation item: the National Natural Science Foundation of China (22168018); the Natural Science Foundation of Jiangxi Province of China (20202BAB204203), and the Natural Science Foundation of Ji'an, Jiangxi Province of China (2021-8-8)

Biographies: HUANG Jing-ping (1980-), male, Nanchang Jiangxi Province, lecturer, MS., Major in electrochemical properties

(E-mail: huangjingping@ganfengbattery.com);

Corresponding author: \*GUO Jin (1979-), female, Ji'an Jiangxi Province, lecturer, MS., Major in electrochemical properties (E-mail: jgsegj@163.com).

## 1 INTRODUCTION

Fossil fuels have brought exponential growth to the human economy, but now mankind is also facing the consequences of this growth containing the climate change, environmental degradation, energy security and a series of problems caused by the depletion of fossil fuels in the next 100 years or so. Driven by the growth of world population and the industrialization process of developing countries, people's desire for energy risen to an unprecedented level compared with the past. Looking forward to the next century, human beings can only place their main energy sources on solar energy and wind energy. However, considering the intermittent and regional characteristics of solar energy and wind energy, in order to make full use of the electric energy generated by them, efficient energy storage devices are very important. In recent years, as an energy storage device, supercapacitor has the characteristics of high power density, long cycle life and fast charge and discharge speed, which has attracted extensive attention of scientific researchers<sup>[1-6]</sup>.

Because of their special chemical and physical properties and many potential applications, inorganic organic hybrid complex materials have attracted extensive attention, such as catalysis, gas storage and separation, sensors, lithium-ion batteries, magnetic and optical properties. The application of inorganic organic hybrid complex materials in the field of supercapacitors has also begun to attract the attention of scientists<sup>[7-12]</sup>.

Base on the special interest in carboxylic acid derivatives, we synthesized an inorganic organic hybrid material with supramolecular structure and investigated its electrochemical properties as super-capacitor electrode materials. The title complex electrode has high specific capacitance, good cycle stability and magnification performance. In 1 mol/L KOH solution, when the current density is 0.5 A/g, the specific capacitance of the electrode reaches 69 F/g.

## 2 EXPERIMENTAL

### 2.1 General procedure

All electrochemical tests were carried out at room temperature using CHI660D electrochemical workstation produced by Shanghai Chenhua Co., Ltd. Using a conventional three electrode system, the foam nickel electrode was used as the working electrode, the Graphite rod as the auxiliary electrode (the counter electrode), the Ag/AgCl as the reference electrode, and the electrolyte is the 1 mol/L KOH solution. The electrodes were tested by cyclic voltammetry (CV) at a scanning rates from 5 to 200 mV/s in the potential range of 0.1 ~ 0.5 V (vs Ag/AgCl); In the potential range of 0.5 ~ 5 V, the electrode was tested by constant current charge discharge (GCD) at different current densities of 1 ~ 20 A/g, and the long-term cycle stability was tested for 5000 cycles at a current density of 5 A/g using a battery testing system (CT3001A, LAND, China); The AC impedance is tested at open circuit potential with an amplitude of 5 mV and in the frequency from 100 mHz to 100 kHz. The specific capacity of the electrode material is calculated by the following formula (1):  $C = I\Delta t / (m\Delta V)$  (1), where C is the specific capacity (F/g), and I is the discharge current of the electrode active material current (A), t is the discharge duration of constant current charge and discharge (s), and m is the mass of the copper base of the material of the active electrode (g),  $\Delta V$  is the potential window (V).

All reactants of A.R. grade were commercially obtained and used without further purification. The infrared spectrum was measured on a PE Spectrum-One FT-IR spectrophotometer over the frequency range 4000~400  $\text{cm}^{-1}$  by using the KBr pellet technique. The photoluminescence of solid-state samples was investigated using LS55 fluorescence spectrometer by Perkin-Elmer company of the United States.

### 2.2 Preparation of the title complex

The title copper complex was prepared by mixing  $\text{CuCl}_2 \cdot 2\text{H}_2\text{O}$  (1 mmol, 175 mg), 5-Nitro-isophthalic

acid (1 mmol, 211 mg), Phen (2 mmol, 360 mg), NaOH (2 mmol, 80 mg) and distilled water (20 mL) were mixed in a 25 mL Teflon-lined stainless-steel autoclave. The mixture was heated to 353 K and kept at this temperature for three days. After cooling the mixture slowly down to room temperature, greenish crystals suitable for X-ray analysis were collected and washed. Yield: 85% (based on copper). IR (KBr,  $\text{cm}^{-1}$ ): 3783 (w), 3451 (vs), 1715 (vs), 1631 (vs), 1534 (s), 1469 (w), 1355 (m), 1287 (m), 1213 (m), 1176 (w), 1104 (w), 778 (w), 729 (m), 664 (s), as presented in Fig. 1.

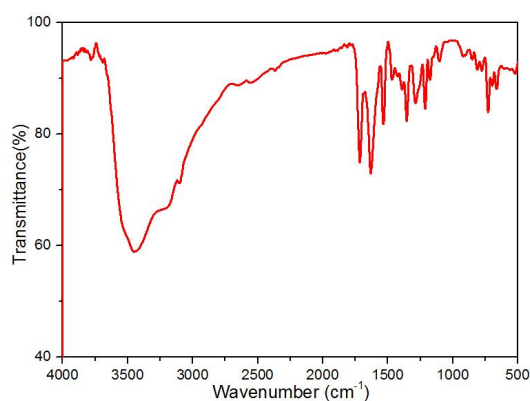


Fig. 1 FTIR spectra of the title complex

The strong absorption peak of the compound in  $\sigma = 3300\text{--}3500 \text{ cm}^{-1}$  is  $3451 \text{ cm}^{-1}$ , which is the characteristic peak of the carboxylate. The strong absorption peak in  $\sigma = 1705\text{--}1725 \text{ cm}^{-1}$  region is  $1715 \text{ cm}^{-1}$ , which is the characteristic peak of the keto group. The peaks of  $1631, 1534, 1469 \text{ cm}^{-1}$  are caused by the stretching vibration of the skeleton of the aromatic ring. At  $\sigma = 1080\text{--}1300 \text{ cm}^{-1}$  and  $\sigma = 1180\text{--}1360 \text{ cm}^{-1}$ , there are multiple asymmetric stretching vibration wave numbers. At  $1099 \text{ cm}^{-1}$ ,  $\sigma = 1080\text{--}1300 \text{ cm}^{-1}$ , and at  $1149 \text{ cm}^{-1}$ ,  $\sigma = 1180\text{--}1360 \text{ cm}^{-1}$ , carbon and oxygen single bonds can be identified.  $1386 \text{ cm}^{-1}$  in the region of  $\sigma = 600\text{--}1500 \text{ cm}^{-1}$ , it can be determined that the compound contains carbon-carbon single bond, as shown in Fig. 1.

### 2.3 X-ray structural determination

The diffraction data were collected on a SuperNova CCD X-ray diffractometer using carefully selected single crystals of the title complex. The X-ray source was graphite monochromated Mo- $K\alpha$  radiation

( $\lambda = 0.71073 \text{ \AA}$ ) and  $\omega$  scan method was employed. The reduction and empirical absorption correction of diffraction data were carried out with the CrystalClear software. Using Olex2<sup>[13]</sup>, the structures of the title complex were solved with the ShelXT<sup>[14]</sup>, the structure solution program using Intrinsic Phasing and refined with the ShelXL<sup>[15]</sup> refinement package using Least Squares minimization. All of the non-hydrogen atoms were generated based on the subsequent Fourier difference maps and were refined anisotropically. The hydrogen atoms, except for the lattice water, were located theoretically and ride on their parent atoms. Reflections measured are 12613; the final  $R = 0.0554$  for 428 parameters and 5600 observed reflections with  $I > 2\sigma(I)$  and  $wR = 0.1434$ , index ranges are  $-12 \leq h \leq 12$ ,  $-15 \leq k \leq 14$ ,  $-14 \leq l \leq 15$ ,  $S = 1.098$ ,  $(\Delta\sigma)_{\max} = 0.99$  and  $(\Delta\sigma)_{\min} = -0.44 \text{ e/\AA}^3$ . A summary of the crystallographic data, and the selected bond distances and bond angles of the title complex are shown in Table 1 and Table 2, respectively.

Table 1 Crystallographic data and structural analysis for the title complex

Empirical formula	$\text{C}_{32}\text{H}_{24}\text{ClCuN}_5\text{O}_8$
Formula weight	704.54
Temperature/K	273
Crystal system	triclinic
Space group	$P\bar{1}$
$a/\text{\AA}$	10.4044(5)
$b/\text{\AA}$	12.3912(9)
$c/\text{\AA}$	12.4632(9)
$\alpha/^\circ$	73.859(6)
$\beta/^\circ$	85.036(5)
$\gamma/^\circ$	78.202(5)
Volume/ $\text{\AA}^3$	1510.09(17)
Z	2
$\rho_{\text{calc}}/\text{cm}^3$	1.549
$\mu/\text{mm}^{-1}$	0.874
F(000)	720.0
Crystal size/ $\text{mm}^3$	$0.22 \times 0.18 \times 0.14$
Radiation	MoK $\alpha$ ( $\lambda = 0.71073$ )
$2\theta$ range for data collection/ $^\circ$	6.772 to 50.998
Index ranges	$-12 \leq h \leq 12, -15 \leq k \leq 14, -14 \leq l \leq 15$
Reflections collected	12613
Independent reflections	5600 [ $R_{\text{int}} = 0.0248, R_{\text{sigma}} = 0.0398$ ]
Data/restraints/parameters	5600/0/428
Goodness-of-fit on $F^2$	1.098
Final R indexes [ $I \geq 2\sigma(I)$ ]	$R_1 = 0.0554, wR_2 = 0.1434$
Final R indexes [all data]	$R_1 = 0.0718, wR_2 = 0.1547$
Largest diff. peak/hole / $\text{e \AA}^{-3}$	0.99/-0.44

**Table 2 Selected bond lengths (Å) and bond angles (°)**

Bond	Dist.	Bond	Dist.	Bond	Dist.
Cu(1)-Cl(1)	2.2883(12)	Cu(1)-N(1)	2.175(3)	Cu(1)-N(2)	1.995(3)
Cu(1)-N(3)	1.990(3)	Cu(1)-N(4)	2.086(3)		
Angle	(°)	Angle	(°)	Angle	(°)
N(1)-Cu(1)-Cl(1)	111.76(9)	N(2)-Cu(1)-Cl(1)	90.75(10)	N(1)-Cu(1)-N(2)	79.74(12)
N(2)-Cu(1)-N(4)	97.04(13)	N(3)-Cu(1)-Cl(1)	94.50(11)	N(3)-Cu(1)-N(1)	95.44(12)
N(3)-Cu(1)-N(2)	173.92(13)	N(3)-Cu(1)-N(4)	80.98(14)	N(4)-Cu(1)-Cl(1)	138.97(9)
N(4)-Cu(1)-Cl(1)	109.27(12)				

### 3 RESULTS AND DISCUSSION

#### 3.1 Single-crystal X-ray diffraction analysis of the title complex

Single-crystal X-ray diffraction analysis revealed the title complex is a neutral molecule that crystallizes in the *P*-1 space group, triclinic system. The asymmetric unit contains one Cu (II) ion, one chloride ion, one 5-nitro-isophthalic acid anion, two Phen molecules and two lattice water molecules. The Cu<sup>2+</sup> ion is coordinated by four nitrogen atoms and one chloride ion, of which four oxygen atoms are from two Phen ligands, forming [CuClPhen<sub>2</sub>]<sup>+</sup> positive ion, a deformed pentapyramid is formed with copper atom as the center, as shown in Fig 2. The following bond distances were observed: Cu(1)-Cl(1) 2.2883(12) Å, Cu(1)-N(1) 2.175(3) Å, Cu(1)-N(2) 2.1995(3) Å, Cu(1)-N(3) 1.990(3) Å, Cu(1)-N(4) 2.086(3) Å. These are comparable with those reported in the literature<sup>[16,17]</sup>. Additionally, there are abundant offset face-to-face  $\pi \cdots \pi$  stacking interactions between Cg1 $\cdots$ Cg4 (symmetry codes: 2-x, 1-y, 1-z), Cg1 $\cdots$ Cg7 (symmetry codes: +x, +y, +z), Cg2 $\cdots$ Cg6 (symmetry codes: 1-x, 1-y, 2-z), Cg4 $\cdots$ Cg4 (symmetry codes: 2-x, 1-y, 1-z), Cg4 $\cdots$ Cg7 (symmetry codes: +x, +y, +z), Cg5 $\cdots$ Cg6 (symmetry codes: 1-x, 1-y, 2-z), Cg7 $\cdots$ Cg7 (symmetry codes: +x, +y, +z), (Cg1 is the ring consisting of C4 to C9; Cg2 is C16 to C21; Cg3 is N2, C1 to C5; Cg4 is N1, C6 to C12; Cg5 is N3, C13 to C17; Cg6 is N4, C18 to C19 and C22 to C24; Cg7 is C25 to C30). The centroid-centroid distance of Cg1 $\cdots$ Cg4 is 3.792 Å, with a slippage distance of

1.492 Å and with a dihedral angle of 1.171; The centroid-centroid distance of Cg1 $\cdots$ Cg7 is 3.633 Å, with a slippage distance of 0.722 Å and with a dihedral angle of 5.742°; The centroid-centroid distance of Cg2 $\cdots$ Cg6 is 3.568 Å, with a slippage distance of 1.015 Å and with a dihedral angle of 1.568; The centroid-centroid distance of Cg4 $\cdots$ Cg4 is 3.907 Å, with a slippage distance of 1.729 Å and with a dihedral angle of 0; The centroid-centroid distance of Cg4 $\cdots$ Cg7 is 3.941 Å, with a slippage distance of 1.677 Å and with a dihedral angle of 6.618°; The centroid-centroid distance of Cg5 $\cdots$ Cg6 is 3.794 Å, with a slippage distance of 1.577 Å and with a dihedral angle of 4.539; The centroid-centroid distance of Cg7 $\cdots$ Cg7 is 3.638 Å, with a slippage distance of 1.402 Å and with a dihedral angle of 0°. In the title complex, the abundant  $\pi \cdots \pi$  stacking interactions yield the 2-D structure, as shown in Fig. 3. In the title complex, there are  $\pi \cdots \pi$  stacking interactions, van der Waals and hydrogen bonds attraction yielding the 3-D supramolecular structure, the crystal packing is presented in Fig.4.

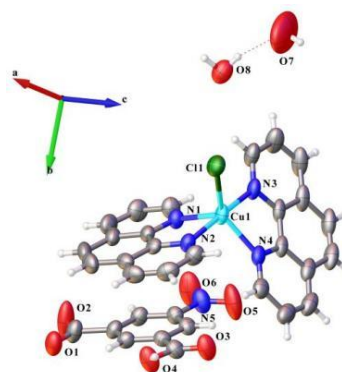


Fig. 2 The crystal structure of the title complex with 50% thermal ellipsoids

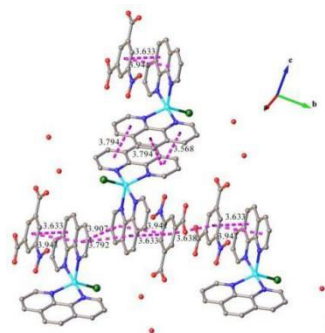


Fig. 3 The  $\pi \cdots \pi$  stacking interaction diagram of the title complex Hydrogen atoms are omitted for clarity

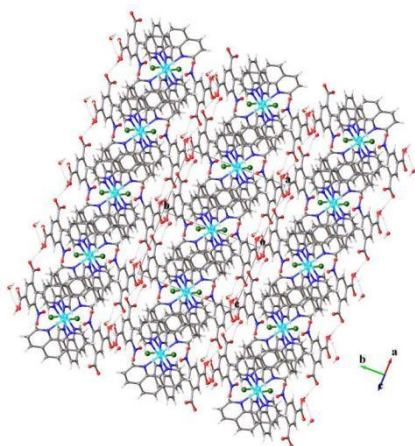


Fig. 4. The packing diagram of the title complex

### 3.2 Electrochemical properties of the title complex

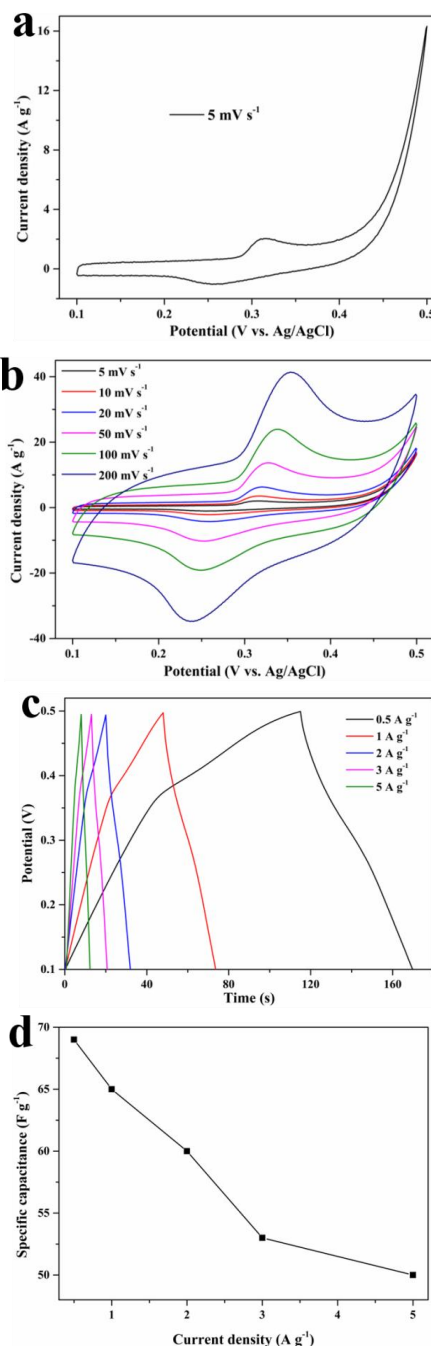
Base on the consideration, increasing attention has been paid to the electrochemical properties of coordination complexes, we conducted CV and GCD analysis in the three electrode system. In 1 mol/L KOH solution, a pair of obvious redox peaks appear in the CV curve of the electrode when the scanning speed is 5 mV/s, indicating that this a pseudo capacitance behavior, as shown in Fig. 5a. Similar precesses have been reported in the other MOFs based electrical materials  $[\text{KCo}_7(\text{OH})_3(\text{ip})_6(\text{H}_2\text{O})_4] \cdot 12\text{H}_2\text{O}$ <sup>[16-18]</sup>.

When the scanning rate of 5, 10, 20, 50, 100, 200 mV/s, with the increase of scanning speed, the positions of the oxidation and reduction peaks move to the positive and negative directions respectively (Fig. 5b), which may be related to the increase of electrode internal resistance. However, the shapes of CV curves are well maintained, indicating good high-rate capability of the as-prepared materials.

At the same time, we investigated the GCD curves of the electrode in 1 mol/L KOH solution, 0.1 ~ 0.5 V charge discharge potential range and different current densities (0.5 ~ 5 A/g), as shown in Fig 5c. As can be seen from Fig 5c, each discharge curve has a slope, indicating that the electrode has undergone redox reaction and generated pseudo capacitance.

The specific capacitance of the title complex electrode calculated according to the discharge curve under different current densities in shown in Fig. 5d. When the current density is 0.5 A/g, the title complex has a high specific capacitance (69 F/g). Even at 5 A/g,

the specific capacitance is about 50 F/g, showing excellent magnification performance. Fig. 5d shows that the specific capacitance decreases with the increase of current density, mainly because the effective interaction between electrolyte ions and electrode materials decreases<sup>[19-20]</sup>.



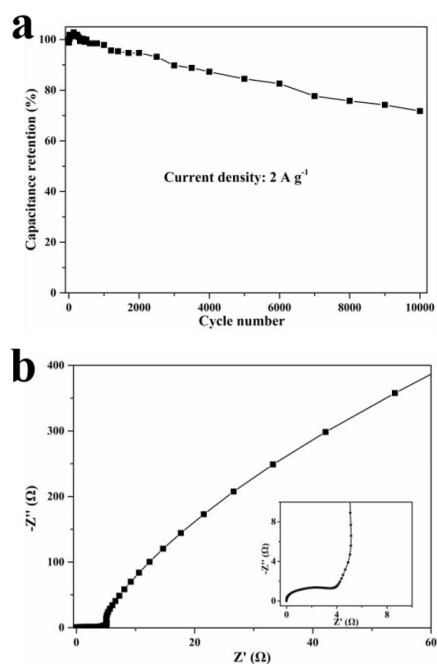
(a) CV curve at the scan rate of 5 mV/s; (b) CV curves at different scanning rates; (c) GCD profiles at different current densities; (d) Relationship between specific capacitance and current density

Fig. 5 Electrochemical properties of Cu-based the title complex in 1 mol/L KOH

Cycle stability is also an important index to investigate the practical application of supercapacitors. When the current density was 2 A/g, the copper based complex electrode was cycled for 10000 times, the capacitance retention was 72%, indicating that the electrode material has good cycling performance, as shown in Fig 6a.

### 3.3 Electrochemical impedance spectroscopy (EIS) of the title complex

Electrochemical impedance spectroscopy (EIS) is also an important index to evaluate electrochemical performance. Fig. 6b is an EIS spectrum under open circuit voltage, which is composed of a semicircle in the high frequency region and a straight line in the low frequency region generated by Faraday reaction. From the semicircle and real axis intercept in the high frequency region (inset in Fig.6), we can know that the internal resistance  $R_s$  of the electrode is about 0.14  $\Omega$ , indicating that it has a small internal resistance at the open circuit potential. The internal resistance is caused by the ion resistance of the electrolyte, the internal resistance of the active material and the contact resistance between the active material and the collector.



(inset, the close-up view of the high-frequency region)

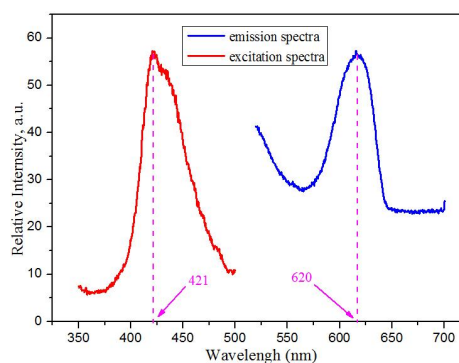
Fig. 6 (a) Cycle performance of Cu-based title complex electrode; (b) EIS spectrum of Cu-based electrode

### 3.4 Photoluminescence property of the title complex

As a typical d9 transition metal coordination polymer, the title complex exhibits potential photoluminescence property<sup>[21-22]</sup>. In order to reveal the potential photoluminescence spectra of the title complex, the photoluminescence spectra was tested for solid-state samples of the title complex and the precursor at room temperature and the results were shown in Fig. 7 and Fig. 8, respectively.

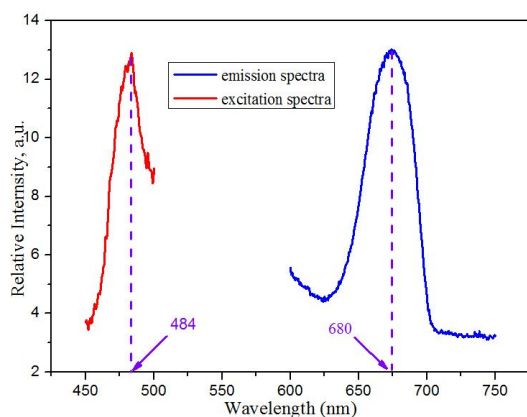
As can be seen from the Fig. 7, it is obvious that the photoluminescent spectrum of complex displayed an effective energy absorption in a wavelength range of 350–500 nm. Upon the emission of 620 nm, the excitation spectrum showed a band at 421 nm. Upon excitation at 421 nm, the emission spectrum was characterized by a sharp band at 620 nm in the orange region. As a result, the precursor of title complex (5-Nitro-isophthalic acid) is a potential orange photoluminescent material.

However, as can be seen from the Fig. 8, it is obvious that the photoluminescent spectrum of complex displayed an effective energy absorption in a wavelength range of 450~ 500 nm. Upon the emission of 680 nm, the excitation spectrum showed a band at 484 nm. Upon excitation at 484 nm, the emission spectrum was characterized by a sharp band at 680 nm in the red region, which is a potential red photoluminescent material. The result is caused by the charge transition in the title complex.



(red curve: excitation; blue curve: emission)

Fig.7 Solid-state photoluminescence spectra of the precursor (5-Nitro-isophthalic acid)



(red curve: excitation; blue curve: emission)

Fig.8 Solid-state photoluminescence spectra of the title complex

## 4 CONCLUSION

In summary, a supramolecular copper complex has been prepared through a hydrothermal reaction and characterized by single-crystal X-ray diffraction. The complex shows high specific capacitance, good cycle stability and excellent rate performance. Specifically, the maximum specific capacitance can achieve 69 F/g in 1 mol/L KOH solution. At the current density of 2 A/g, the retention of specific capacitance was 72% after 5000 cycles. At the same time, the title complex is a potential red photoluminescent material.

Further investigations on the relationship between the structure and the properties of copper crystalline complex are in progress in our laboratory.

### Supplementary Materials

Crystallographic data for the structural analysis have been deposited with the Cambridge Crystallographic Data Center, CCDC No. **2168480**. Copies of this information can be obtained free of charge from the Director, CCDC, 12 Union Road, Cambridge, CB2 1EZ, UK (fax: +44-1223-336033); email: [deposit@ccdc.cam.ac.uk](mailto:deposit@ccdc.cam.ac.uk) or online at <http://www.ccdc.cam.ac.uk>.

### Declarations

Conflict of interest on behalf of all authors, the corresponding author states that there is no conflict of interest.

## REFERENCES:

- [1] Xu P, Liu J, Huang J H, et al. Interfacial engineering of CuSCN-based perovskite solar cells via PMMA interlayer toward enhanced efficiency and stability[J]. *New Journal of Chemistry*, 2021, 45(29): 13168-13174.
- [2] Yang Y N, Zhou Y N, Ouyang B, et al. Influence of thermal runaway in styrene-acrylonitrile bulk copolymerization revealed by computational fluid[J]. *AIChE Journal*, 2022, 68(5):e17645.
- [3] Quader A, Mustafa G M, Abbas S K, et al. Efficient energy storage and fast switching capabilities in Nd-substituted  $\text{La}_2\text{Sn}_2\text{O}_7$  pyrochlores[J]. *Chemical Engineering Journal*, 2020,396:125198.
- [4] Zhu L T, Lei H, Ouyang B, Luo Z H. Using mesoscale drag model-augmented coarse-grid simulation to design fluidized bed reactor: Effect of bed internals and size[J]. *Chemical Engineering Science*, 2022,253:117547.
- [5] Li X W, Ma N, Xu G T, et al. Efficient electrochromic device employing thermal tolerant hydrogel electrolyte with a wide operating temperature range from  $-40$  to  $60$  °C [J]. *Solar Energy Materials and Solar Cells*, 2022, 234: 111449.
- [6] Chen H J, Lyu G Y, Yue Y F, et al. Improving the photovoltaic performance by employing alkyl chains perpendicular to the  $\pi$ -conjugated plane of an organic dye in dye sensitized solar cell[J]. *Journal of Materials Chemistry C*, 2019,7:7249-7259.
- [7] Yi X G, Liu Y Z, Fang X N, et al. Crystal structure and properties of  $[\text{PrCl}(\text{H}_2\text{O})_3(\text{L})(\text{HL})]_n\text{Cl}$  (HL = 3-hydroxy-2-methylquinoline-4-carboxylic acid) with one-dimensional chains[J]. *Chinese Journal of Inorganic Chemistry*, 2019, 38:325-330.
- [8] Shi H, Zhao F F, Chen X H, et al. Colorimetric and ratiometric sensors derivated from natural building blocks for fluoride ion detection[J]. *Tetrahedron Letters*, 2019, 60: 151330-151334.
- [9] Wang W Y, Chen H J, Yue Y F, et al. Electropolymerization of V-shape D-A-D type monomers for efficient and tunable electrochromes[J]. *Dyes and Pigments*, 2021,194: 109615.
- [10] Fu W A, Chen H J, Han Y Y, et al. Electropolymerization of D-A-D type monomers consisting of triphenylamine and substituted quinoxaline moieties of electrochromic devices[J]. *New Journal of Chemistry*, 2021,45:19082-19087.
- [11] Xing J N, Shu M, Wang W Y, et al. Synthesis and properties of electrochromic material based on phenanthroline Fe(II) complex with triphenylamine

- moiety[J]. Chinese Journal of Inorganic Chemistry, 2021, 37(10):1847-1852.
- [12] Jeffrey C, David R B, Li L, et al. Hybrid time-domain and continuous wave diffuse optical tomography instrument with concurrent, clinical magnetic resonance imaging for breast cancer imaging[J]. Journal of Biomedical Optics, 2019,24:051409-051420.
- [13] Dolomanov O V, Bourhis L J, Gildea R J. Olex2: a complete structure solution, refinement and analysis program[J]. Journal of Applied Crystallography, 2009, 42:339-341.
- [14] Sheldrick G M. A short history of SHELX[J]. Acta Crystallographica A, 2008, 64(1):112-122.
- [15] Sheldrick G M. Crystal structure refinement with SHELXL[J]. Acta Crystallographica C, 2015,71:3-8.
- [16] Xiao H P, Li X H, Cheng Y Q. Catena-(( $\mu$ -2-5-nitroisophthalato)-2,2'-bipyridine-copper(II)[J]. Acta Crystallographica, E: Rep. Online,2005,61(4):158.
- [17] Wang Y F, Yi X G, Fang X N, et al. Hydrothermal preparation, crystal structure photophysical properties and theoretical calculation of a Cu(II) complex[J].Journal of Chemical Crystallography, 2021,51(2):169-174.
- [18] Rong H R, Wang X M, Ma Y W, et al. Three-dimensional cobalt-based MOF  $[\text{KCo}_7(\text{OH})_3(\text{ip})_6(\text{H}_2\text{O})_4] \cdot 12\text{H}_2\text{O}$  as high-capacity electrode materials for supercapacitors[J]. Chinese Journal of Inorganic Chemistry, 2021,37(1):206-212.
- [19] Zhong J H, Wang A L, Li G R, et al.  $\text{Co}_3\text{O}_4 / \text{Ni}(\text{OH})_2$  composite mesoporous nanosheet networks as a promising electrode for supercapacitor applications[J]. Journal of Materials Chemistry, 2012, 22(12):5656-5665.
- [20] Ersozoglul M G, Gilsing H D, Gencturk A, et al. A novel dioxithiophene based conducting polymer as electrode material for supercapacitor application[J].International Journal of Electrochemical Science,2019,14(9):9504-9519.
- [21] Chen H H, Yi X G, Pan C W, et al. Hydrothermal preparation and photophysical properties of a Ni(II) complex containing quinoline derivative and Phen ligands[J]. Chinese Journal of Structural Chemistry, 2021,40(4):501-506.
- [22] Yi X G, Fang X N, Wang Y F, et al. Synthesis, characterization, properties, and theoretical calculation of an inorganic-organic hybrid mononuclear copper (II) complex containing 3- hydroxy - 2 - methyl- quinoline -4- carboxylate[J]. Journal of Chemical Crystallography, 2020, 50(4):348-356.